Analyst

Accepted Manuscript

ROYAL SOCIETY OF CHEMISTRY

www.rsc.org/analyst

Journal Name

ARTICLE

An in solution assay for interrogation of affinity and rational minimer design for small molecule-binding aptamers

Received 00th January 20xx,
Accepted 00th January 20xx

DOI: 10.1039/x0xx00000x

www.rsc.org/

Nadine R. Frost,[a] Maureen McKeague,[a,b] Darren Falcioni[a] and Maria C. DeRosa*[a]

Aptamers are short single-stranded oligonucleotides that fold into unique three-dimensional structures, facilitating selective and high affinity binding to their cognate targets. It is not well understood how aptamer-target interactions affect regions of structure in an aptamer, particularly for small molecule targets where binding is often not accompanied by a dramatic change in structure. The DNase I footprinting assay is a classical molecular biology technique for studying DNA-protein interactions. The simplest application of this method permits identification of protein binding where DNase I digestion is inhibited. Here, we describe a novel variation of the classical DNase I assay to study aptamer-small molecule interactions. Given that DNase I preferentially cleaves duplex DNA over single-stranded DNA, we are able to identify regions of aptamer structure that are affected by small molecule target binding. Importantly, our method allows us to quantify these subtle effects, providing an in solution measurement of aptamer-target affinity. We applied this method to study aptamers that bind to the mycotoxin fumonisin B_1, allowing the first identification of high affinity putative minimers for this important food contaminant. We confirmed the binding affinity of these minimers using a magnetic bead binding assay.

Introduction

Aptamers are short, single-stranded oligonucleotides that are selected to bind with high affinity and selectivity to a target. Aptamers have many advantages over traditional molecular recognition elements, including antibodies. For example, chemical modifications can be introduced at precise sequence locations during their chemical synthesis. Furthermore, aptamers are stable and reversibly denatured by heat. As they are selected in vitro and do not require animals or cell culture, aptamers can be generated against toxic compounds or those that do not elicit an immune response.[1] Aptamers fold into three-dimensional conformations producing unique binding sites for aptamers to act as ligands for large molecules, or conversely act as receptors for small molecules. Given this versatility, aptamers are well suited for a range of biosensor applications.[1]

Generally, the quality of an aptamer is evaluated through its binding affinity, using the dissociation constant (K_d). There are few K_d methods that can be considered universally applicable for all types of target molecules. Furthermore, measuring the K_d for aptamers binding small molecules is a challenge as many of the established K_d quantification techniques are separation- or mass-based techniques (ie: equilibrium dialysis, SPR, AFM, HPLC etc.), or alternatively rely on inherent fluorescence or absorption properties of the target.[2-4] A limited number of techniques are available that yield structural and/or thermodynamic information of aptamer interactions with small molecules, such as circular dichroism and isothermal titration calorimetry.[5,6] As a result, K_d determination of small molecule targets often relies on tethering the target and/or aptamer to a surface, which can result in compromised binding.[2] In many cases, the measured K_d may vary based on the chosen technique. Therefore, it is valuable to develop aptamer characterization methods that use conditions analogous to those anticipated in the downstream application. Rapid methods for measuring aptamer affinity are limited and thus screening and determination of K_d remains a bottleneck in aptamer-based biosensor development for many important small molecule targets.

Another important characteristic to evaluate for an aptamer is its structure; characterizing DNA structure is vital to understanding and predicting interactions between DNA and other molecules.[7] The structure of aptamers is based on duplex, triplex, or quadruplex formation between complementary nucleotides in the primary sequence. There are several approaches to determining the structure of an aptamer. As a starting point, computational programs predict the most stable structure based on the lowest free energy. For example, the RNA Structure webserver predicts the secondary structure of RNA or DNA sequences based on thermodynamic parameters and probability of base pair interactions to form

[a] Chemistry Department, Carleton University, 1125 Colonel By Drive, Ottawa, ON, Canada, K1S 5B6
[b] Present address: Department of Bioengineering, Stanford University, 443 Via Ortega, Stanford, CA, 94305
* To whom all correspondence should be addressed: maria.derosa@carleton.ca
Electronic Supplementary Information (ESI) available: Additional studies, controls, and experimental details. See DOI: 10.1039/x0xx00000x

the most likely secondary structure.[8-10] However, these predictions do not always accurately reflect nucleic acid structure and must be verified experimentally. Furthermore, they are limited to the evaluation of the nucleic acid sequence alone and cannot take into account any interactions with a target molecule. Unfortunately, there are limited techniques to experimentally map the structure of a DNA sequence. NMR spectroscopy and X-ray crystallography are the gold standard, however these can be labour intensive and are therefore not practical for screening of multiple aptamer sequences.[7,11-13]

DNase I footprinting is a classical molecular biology technique that was developed to study the binding of regulatory proteins to DNA. DNase I is an endonuclease that cleaves DNA to produce 5'-phosphorlyated di-, tri-, and oligonucleotide fragments.[14] Using the digestion of DNase I on genomic DNA, footprinting assays map protein binding sites on ^{32}P-labeled DNA and examine structural changes in the DNA upon protein binding.[14] In a protection assay, DNA is labelled at one terminus. Binding of regulatory proteins protects the phosphodiester backbone from cleavage by DNase I resulting in regions with no fragments, producing the "footprint" of the binding site(s) when fragments are separated by gel electrophoresis.[15-17] This technique generates structural and thermodynamic information at the site(s) of protein interaction. A concentration-dependent protection generates a binding isotherm, allowing quantification of binding affinity.[15] Since its initial invention, many variations have been applied resulting in improved resolution or obtaining sequence specific information for a variety of important protein-DNA interactions.[18-21] While DNase I footprinting has been used to discern the binding sites of aptamers for large targets such as proteins and bacteria,[19-22] it has not been explored to map the secondary structure of aptamers, nor to characterize the subtle changes in secondary structure that result upon aptamer-target binding. While the unique secondary structure of an aptamer facilitates its selective binding to a target, small molecule binding may not necessarily be accompanied by large conformational change. Therefore, target binding would not be expected to mask or protect large portions of a sequence as observed with proteins.[22] As a result, aptamer binding sites arising from small molecules are more difficult to map and less understood.

An alternative method for examining aptamer structure was first reported by Burgstaller *et al* (1995). In this method, they used chemical probes (DMS, kethoxal, and CMCT) to react at various nucleotides within the sequence. Binding of the small molecule target inhibited the structure probe binding and generated a "footprint" at binding sites in the ^{32}P-labeled cDNA. This method was useful for mapping binding sites in aptamers, however these chemicals show bias in their reaction to each nitrogenous base.[23] Therefore, this method may not always be generally applicable to certain nucleotide-rich aptamers. A simplified alternative to this approach that could be used for the facile comparison and screening of aptamer sequences would be advantageous. We hypothesized that the DNase I assay could be applied to probe aptamer structure upon target binding and that this assay would not be biased to certain residues. As DNase I digests double stranded DNA with a significantly higher efficiency (~1000x greater) than single stranded DNA, a digestion profile of aptamers that is directly related to their structure may be elucidated.[14]

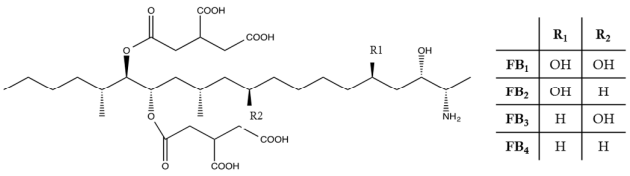

	R_1	R_2
FB_1	OH	OH
FB_2	OH	H
FB_3	H	OH
FB_4	H	H

Figure 1. The major fumonisins (FB_1 – FB_4) showing slight structural variations in the position and number of hydroxyl residues. Non-covalent interactions between FB_1 and *FB_1 39* can include van der Waals forces, hydrophobic effects, electrostatic interactions, etc.

We performed this work in the context of aptamers that bind to the small molecule mycotoxin, fumonisin B_1 (FB_1). The fumonisin toxins (predominantly FB_1, FB_2, and FB_3) are produced by *Fusarium verticilloides* and *F. proliferatum,* common fungal contaminants of maize (Figure 1).[24,25] FB_1 is toxic by consumption; leukoencephalomalacia is observed in horses, pulmonary edema in swine, and nephrotoxicity and carcinogenicity in rodents.[26] In humans, FB_1 is also implicated in neural tube and craniofacial defects.[27] Regulation of FB_1 on maize crops is important globally to mitigate human and animal toxicity, and to harmonize regulatory thresholds that have a significant economic effect on the global food trade.[28] Current analytical techniques for regulating FB_1 include high performance liquid chromatography (HPLC)[29-30] and enzyme-linked immunosorbant assays (ELISA).[31-33] These methods require skilled technicians and advanced laboratory equipment. The development of rapid, inexpensive methods for the detection of contaminations in food and feed in the field might mitigate the cost, time, and waste with current detection methods. Aptamers for FB_1 could serve as the molecular recognition elements for such simple, portable biosensor technology.

To-date, two aptamer selections have been reported for this target.[34,35] One of these aptamers, *FB_1 39*, has a reported K_d of 100 ± 30 nM (Table 1). This aptamer has been implemented in four different detection systems.[36-39]

DNA aptamer	Sequence (5'-3')	Reported K_d (nM)
FB_1 39	FATACCAGCTTATTCAATTAATCGCATTACCTT ATACCAGCTTATTCAA*TTACGTCTGCACATACC* *AGCTTATTCAATT*AGATAGTAAGTGCAATCT	100 ± 30

Table 1. DNA aptamer sequence for *$FB_1$39*, primer regions are underlined. The sequence of a predicted minimer *FB1_39m3* is in italics. F = 5'-fluroescein. Reported K_d was determined by a magnetic bead binding assay.[31]

FB_1 39 is 96 nucleotides in length, which is relatively long for an aptamer (Table 1). The truncation of an aptamer into shorter sequences, containing only regions involved in binding to the target, is desirable as these "minimers" have in some

cases been shown to bind with higher affinity and are much cheaper to manufacture. Structural information from the DNase I assay may provide useful information that can be leveraged for the rational design of minimers and provide a rapid method for evaluating the K_d of these minimer sequences.

Results and discussion

Design and synthesis of FB_1 39 minimers

The *FB_1 39* aptamer used for this study was selected by McKeague *et al.*[34] Truncated aptamers were synthesized to test their structure and affinity relative to the full-length sequence, e.g., removal of the 3' primer binding region (*FB1_39t3*), removal of the 5' primer binding region (*FB1_39t5*) removal of both primer binding regions (*FB1_39t3-5*), and a region at the 3'-end of the sequence predicted to have a stem loop structure (*FB1_39m3*) (Figure 2). *FB1_39m3* was selected as this region contains the highest degree of predicted stable secondary structure in the stem loop motif. As the interaction between FB_1 and *FB_1 39* is not fully understood, it was decided to test this region to see if it was critical to binding. Also, a "complementary probe displacement region" (orange) is noted as existing FB_1 aptasensors exploit the target binding event to displace a complementary oligonucleotide probe at this location.[37,38] (Figure 2) All aptamers were chemically modified with 5'-fluorescein during synthesis.

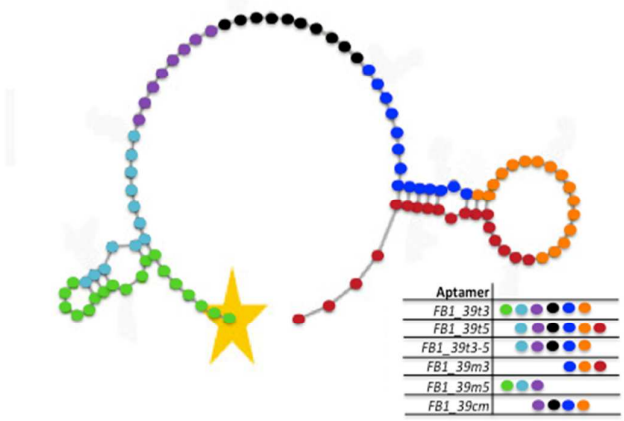

Figure 2 Predicted secondary structure of *FB_1 39* showing minimers: no 3' primer binding region (PBR) (*FB1_39t3*), no 5' PBR (*FB1_39t5*), no PBRs (*FB1_39t3-5*), and 3' stem loop region (*FB1_39m3*) The region used for probe displacement in sensor applications is indicated in orange.[37,38] Additional minimers (FB1_39m5 and FB1_39cm) are included in the SI analysis (SI Fig 3 & SI Fig. 6). The 5'-fluorescein modification is indicated by the yellow star. The aptamer sequence indicating the aforementioned regions is as follows:
5'ATACCAGCTTATTCAATTAATCGCATTACCTTATACCAGCTTATTCAATTACGT CTGCACATACCAGCTTATTCAATTAGATAGTAAGTGCAATCT-3'

Preliminary structural screen using variable temperature UV-Vis analysis (T_m)

All aptamers used in this study were first analysed by variable temperature UV-Visible spectroscopy to determine experimental melting temperatures (T_m). A higher melting temperature is indicative of a greater degree of stable secondary structure. At 260 nm, denatured DNA absorbance is higher than duplex DNA due to hyperchromicity. All T_m graphs are shown in the supporting information (SI Figure 1). The T_m's for *FB_1 39* and *FB1_39t5* were highest (41.0 and 42.9°C respectively). The minimers *FB1_39t3* and *FB1_39t3-5* had significantly lower T_m's (13.3 and 19.1°C respectively) indicating that at room temperature the structures were not all completely formed (SI Figure 1). This suggests that the 3' region of the aptamer is critical in forming the main structure within the *FB_1 39* aptamer sequence.

We compared the RNA structure predictions for each aptamer with the melting temperatures.[8-10] The RNA structure predictions are based on the highest probability of duplex formation within the structure, presenting the structure with the lowest free energy. For each case, the structure predictions and measured melting temperature compared well. In particular, *FB_1 39*, *FB1_39t5*, and *FB1_39m3* have the highest degree of secondary structure with prominent hairpin formation, whereas *FB1_39t3* and *FB1_39t3-5* have significantly less secondary structure predicted. The lowest degree of secondary structure, *FB1_39t3*, corresponds with the lowest experimental T_m (13.3°C) (SI Figure 1). All sequences were also analysed in the presence of 1 µM FB_1 which did not result in any significant changes in T_m (data not shown). This suggests that there were no dramatic changes in structure induced by target binding that could be detected with a standard melting assay.

DNase I assay optimization and screening

To first confirm that patterns of DNase I digestion could be mapped and that structure patterns could be elucidated, three rationally designed single-stranded DNA (ssDNA) sequences were synthesized and subjected to DNase I digestion and the fragments were separated on a 19% denaturing polyacrylamide gel (PAGE). The prominent fragments produced in the digestion that contain the 5'-fluorescein label appear as bands on the gel; these are fragments produced due to DNase I digestion at duplex regions within the sequence. The assay design of this technique is shown in Figure 3. Where the hairpins were predicted within the designed structures, we saw corresponding areas on the gel with increased fragments after digestion. As the digestion patterns matched well with the predicted secondary structures (SI Figure 2), we next explored whether the approach could be applied to the *FB_1 39* aptamer and proposed minimers in the absence and presence of the target. We predicted that target concentration-dependent changes in the DNase I digestion profile would identify areas of the aptamer where duplex regions are stabilized or destabilized due to target binding (Figure 3).

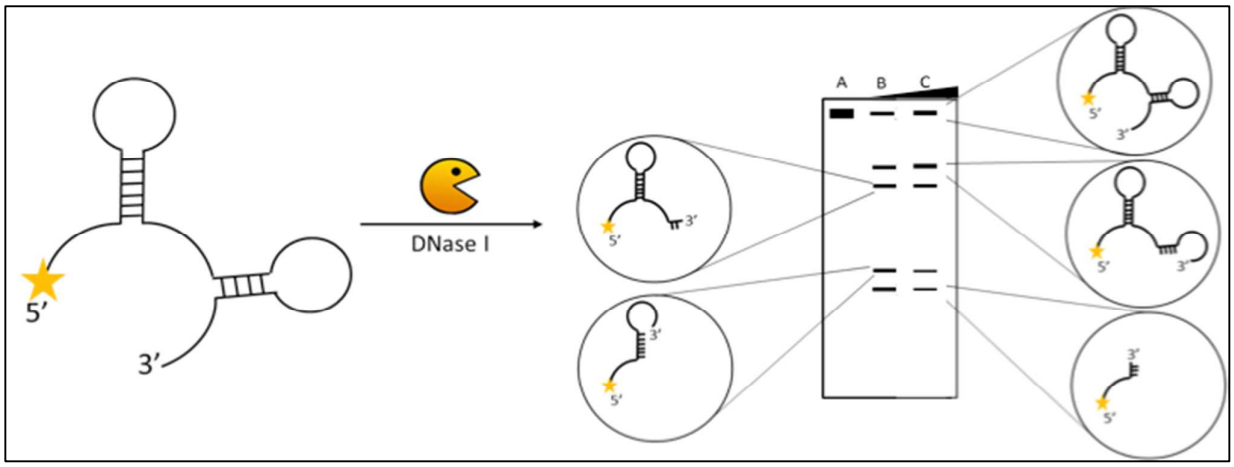

Figure 3. DNA aptamer with a unique secondary structure is tagged with 5'-fluorescein, represented by the yellow star. Digestion by DNase I produces fragments (fluorescently tagged at the 5' end) that are separated by size on a denaturing PAGE gel. Only fragments retaining the label are visualized on the gel. Undigested full-length DNA with no DNase I treatment is shown in lane A, fragmented DNA after DNase I digestion in lane B, and band intensity change due to the subtle effects of target binding is shown in lane C.

Given the high propensity of duplex DNA digestion by DNase I, it is insinuated that regions of duplex structure can be mapped by running a DNase I digestion profile of the aptamer on a PAGE gel. Aptamer concentration and DNase I digestion time were optimized to establish a level of DNase digestion that produced a full spectrum of fragments but did not completely digest the aptamer. The target concentrations were selected to cover the predicted K_d range. Figure 4 and SI Figure 3 present digestion profiles for *FB_1 39* and its minimers, respectively. The digestion fragments near the top of the gel represent digestion at the 3' hairpin (longer sequences labelled with 5'-fluorescein), and the fragments at the bottom are due to digestion at the 5' hairpin (shorter sequences labelled with 5'-fluorescein). The major DNase I digestion bands can be aligned to predicted hairpins within the structure, with a few exceptions. The fragments of *FB_1 39* produced by DNase I digestion correspond with the predicted secondary structure of the sequence. On the other hand, *FB1_39t3* is noted to have the lowest T_m and negligible predicted structure; however, the DNase I digestion assay produces reproducible bands suggesting the presence of duplex DNA under the conditions of the assay, which is limited to buffer conditions suited to DNase I activity (see experimental for details). The most prominent band produced by DNase I digestion, Band E, corresponds to a fragment produced by digestion within the central region of *FB_1 39* where no secondary structure is predicted but where DNase I is able to digest with high propensity (Figure 4, SI Figure1, SI Figure 5).

The objective of the DNase I footprinting assay is to distinguish any subtle changes in aptamer structure that occur upon target binding. We characterized this effect through the change in digestion profile relative to target concentration. Aptamer (50 µM) was incubated in equal volumes with a range of FB_1 concentrations (0 – 10 µM) to quantify the effect of target binding on fragment bands within the DNase I digestion profile. After analysis of the 5'-fluorescein labelled digestion fragments by 19 % denaturing PAGE, the normalized band intensity (intensity of band / total lane intensity, to account for any loading volume discrepancies) was plotted against the log concentration of target, producing a binding isotherm and enabling the calculation of dissociation constant (K_d). Analysis was performed for each aptamer sequence. As the changes in band intensity were subtle, a minimum of six replicates of the assay was performed to ensure confidence in the observed trends (Figure 4).

Given that all regions of the full-length aptamer are likely not directly involved in binding with the target, it was expected that there would be regions of the aptamer where increasing concentrations of target would not impact the digestion pattern or band or the band intensity. To identify the digestion bands of interest, we performed a preliminary analysis of the DNase I digestion using heat maps (SI Figure 3A-D). Bands that exhibited consistent change in intensity relative to the target concentration were then utilized to calculate a binding affinity (K_d). It is expected that the K_d determined from an analysis of each band of the DNase I digestion assay will provide an apparent binding affinity. The K_d of each band represents a local change in digestion propensity, either with target stabilizing or destabilizing the structure in the digestion region. Through interpreting the apparent local K_ds of binding between the full length and minimer sequences, one can acquire a more comprehensive understanding of the global K_d of the aptamer binding to target in solution.

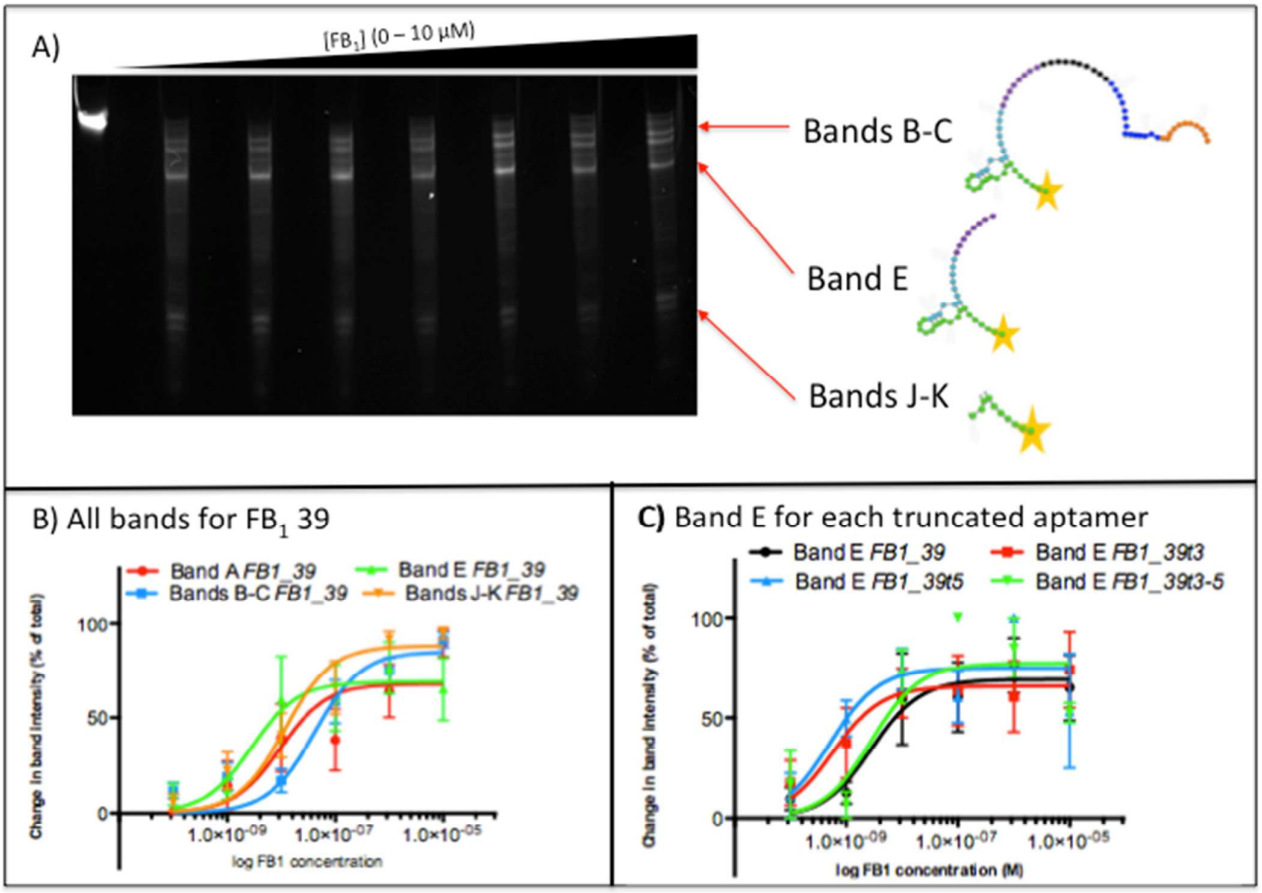

Figure 4. A) DNase I assay for *FB₁ 39* separated by 19% denaturing PAGE, FB_1 concentration range from 0 – 10 µM. The full-length undigested sequence is in the first lane. Prominent bands are indicated with a visual representation of the 5'-fluorescein tagged digestion product after digestion by DNase I. **B)** K_d binding isotherms for each prominent band within the *FB₁ 39* DNase I digestion assay, determined by non-linear regression one-site specific binding analysis on GraphPad Prism. K_ds: Band A (9.6 ± 7.7 nM); Bands B-C (41.8 ± 16.3 nM); Band E (2.8 ± 2.4 nM); Bands J-K (11.6 ± 5.0 nM). **C)** K_d of Band E for *FB₁ 39* (2.8 ± 2.4 nM); *FB1_39t3* (0.6 ± 0.5 nM); *FB1_39t5* (0.5 ± 0.4 nM); *FB1_39t3-5* (2.8 ± 2.7 nM) determined by non-linear regression one-site specific binding analysis on GraphPad Prism. Full analysis of *FB₁ 39* minimers can be found in the supporting information (SI Figure 3).

Measuring aptamer affinity with the DNase I assay

The PAGE gel and K_d analysis for *FB₁ 39* is shown in Figure 4. The corresponding gels and K_d analysis for the *FB₁ 39* minimers are in SI Figure 3. Further analysis of other FB_1 aptamers is also included in the SI to illustrate the applicability of this technique on a variety of aptamers for FB_1 (SI Table 1, SI Figure 4).[31] *FB₁ 39* showed the greatest change in intensity with concentration at the band labelled "E". Digestion at the site producing "Bane E" corresponds to the minimer *FB1_39m5* based on the size of this 5'-fluorescein labelled fragment (calculated by distance travelled on the gel, SI Figure 5). Additionally, band E is the most intense band in the gel, indicating a high propensity of DNase I cleavage at the site producing that fragment. Importantly, we demonstrate that the high binding affinity of the full-length *FB₁ 39* aptamer was retained in the truncated minimers (*FB1_39t3*, *FB1_39t5*, *FB1_39t3-5*) at Band E, a common digestion fragment produced between the sequences. *FB1_39m5* (Band E) and *FB1_39cm* (region surrounding Band E) both demonstrated apparent K_ds with low nM affinity to FB_1 from the DNase I assay (SI Fig 6). However, *FB1_39m3*, the minimer containing the 3' hairpin, did not demonstrate any binding by the DNase I assay, and after DNase I digestion it did not share the common digestion pattern containing Band E (SI Figure 3). While there are digestion bands present on the gel for this sequence, there is no consistent change in band intensity relative to FB_1 concentration, which suggests an absence of binding. This observation confirms that the changes in band intensity, although subtle, correlate with the change in target concentration at positions where binding occurs. If there is no binding, there is no consistent change in band intensity, indicating that this method is reliable for identifying true binding interactions. To further validate this method, we tested the full length *FB₁ 39* sequence with Ochratoxin A, a target for which the aptamer has no affinity. No concentration dependent changes in band intensity could be seen. However, when we performed the same experiment in the presence of FB_2, a structurally similar fumonisin which only differs by the lack of a single OH group at the carbon 11 position, we saw a comparable change in band intensity suggesting that the

aptamer binds FB_2 with similar affinity and that binding has a similar effect on aptamer structure (SI Figure 7).

One drawback of this assay is that because of the subtle nature of the band intensity variations with changing concentration, the errors associated with the K_d are relatively large. Regardless, the assay allows for clear distinction of binding vs. non-binding and more importantly allows for an assessment of binding affinity with target free in solution, rather than tethered to a solid support. While the large errors may currently preclude this method from its use for independent K_d determination, it can be used in conjunction with other methods to confirm binding affinity, validate function, and measure selectivity.

Confirmation using the magnetic bead assay

We next employed a standard magnetic bead binding assay to confirm the relative binding affinity of *FB_1 39* minimers and the full-length *FB_1 39*. McKeague *et al* (2010) used a similar binding assay to determine the K_d of *FB_1 39* to be 100 ± 30 nM.[31] In this assay, the target, FB_1, is covalently bound at a constant concentration to the superparamagnetic beads. A range of aptamer concentrations are incubated with the beads to allow for binding between the aptamer and target. Unbound sequences are washed off, and binding aptamers are eluted with heat and quantified with fluorescence spectroscopy. No aptamer was observed to bind to unmodified beads with no target (data not shown). The K_d values determined from three replicates are shown below for *FB_1 39* and minimers, as well as A08[40] Ochratoxin A control aptamer (SI Figure 8)(Figure 5).

The full length *FB_1 39* sequence bound with the highest affinity of 99 ± 31 nM, in agreement with the affinity determined by McKeague *et al* (2010).[31] Of the minimers, *FB1_39t3* and *FB1_39t3-5* had the highest affinity, also in the nM range. *FB1_39m3* and the A08 control exhibited no binding to FB_1, further confirmation of the results found by the DNase assay. We note that there is almost two orders of magnitude difference in the calculated K_d for these minimers between the two methods (low nM for DNase I vs. high nM for magnetic bead) as summarized in Table 2. This discrepancy may be attributed to the fact that the target in the magnetic bead assay is tethered to a solid support, which could lead to steric hindrance that impedes binding. In any K_d assay, the equilibrium affinity is changed by any modifications to either partner (aptamer, target). The K_d determined is relative to the test conditions and constraints. Alternatively, the amino group used to conjugate FB_1 to the beads may be implicated in improved binding. The primary amine of FB_1 is masked when it is conjugated to magnetic beads similarity to the conditions under which SELEX was performed for *FB_1 39*, indicating that the aptamer is likely interacting with the tricarballyic residues on the FB_1 structure.[34] Regardless, the difference should be interpreted with some caution, given the large variability in the DNase assay values. The comparison between these two methods confirms the ability of the DNase I assay to screen for selective binding.

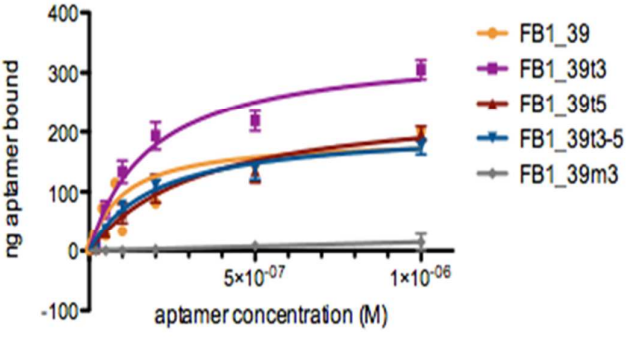

Figure. 5 Magnetic bead affinity assays for *FB_1 39* and minimers. *FB_1 39* (K_d = 99 ± 31 nM); *FB1_39t3* (K_d = 184 ± 43 nM); *FB1_39t5* (K_d = 328 ± 106 nM); *FB1_39t3-5* (K_d = 195 ± 45 nM); *FB1_39m3* (K_d = No Binding). Binding isotherms generated by GraphPad Prism non-linear regression one site specific binding.

Aptamer	DNase I assay (Band E) (nM)	Magnetic Bead Assay (nM)
$FB_1$39	2.8 ± 2.4	99 ± 31
FB1_39t3	0.6 ± 0.5	184 ± 43
FB1_39t5	0.5 ± 0.4	328 ± 106
FB1_39t3-5	2.8 ± 2.7	195 ± 45
FB1_39m3	N.B	N.B

Table 2. Comparison of K_d's of each FB1 aptamer as determined by DNase I assay (Band E) and Magnetic Bead assay. N.B = no binding.

A major advantage of this affinity screening method is that in addition to providing a rapid yes/no answer with respect to target binding, structural information can also be decoded, in particular about which regions in the aptamer are required for binding. In both the DNase I and magnetic bead assay, the minimer composed only of the region of highest predicted secondary structure within the sequence, *FB1_39m3*, did not bind to FB_1 alone. In two sensor applications, the sensing mechanism required a complementary probe (15 – 17 nucleotides long, see Figure 2) to *FB_1 39* that bound to the region adjacent to the 3' primer binding region[34,35] to be displaced by FB_1 binding to yield a signal. This indicates that the region adjacent to the 3' primer binding region is involved in target binding, but in order to retain target binding capacity, the minimers must contain the region further 5' than *FB1_39m3*, such as *FB1_39t3-5.*

Experimental

DNA synthesis and purification

All aptamers were synthesized on a BioAutomation Mermade 6 DNA synthesizer using standard phosphoramidite chemistry. 1000 Å controlled pore glass (CPG) columns were used (BioAutomation), and all aptamers were modified with 5'-fluorescein phosphoramidite (Glen Research). After synthesis, the sequences were cleaved from the beads by incubation with 1 ml 28% ammonium hydroxide at 55°C for three hours followed by 21 hours at room temperature. After

centrifugation to pellet out the beads, the supernatant was transferred to a clean tube. The beads were washed with 1 ml deionized water, centrifuged, and the supernatants were combined and dried overnight on a Savant AE2010 SpeedVac. Aptamers were purified by 12% denaturing polyacrylamide gel electrophoresis (PAGE). After polymerization, the gels were pre-run for 15 minutes at 300 V using a SE 600 Chroma Standard Dual gel electrophoresis unit. DNA samples were dissolved in 350 µl deionized water and 350 µl formamide, heated at 55°C for 5 minutes, and loaded into the gel to run for 100 minutes at 300 V. Gels were visualized with epiUV (excitation 254 nm) and Fluorescence (fluorescein filter) with an AlphaImager Multi Image Light Cabinet (Alpha Innotech). The fluorescent band (5'-fluorescein labelled aptamer) was cut out of the gel and incubated in 20 ml deionized water at 37°C overnight in a New Brunswick Scientific Innova 40 incubation shaker. The solution was filtered through 0.22 µm cellulose acetate syringe filters to remove gel fragments, and dried on a Labconco Freezone lyophilizer. The aptamers were then reconstituted in a minimal volume of deionized water, and passed through Desalting Amicon-Ultra 0.5 ml 3kDa centrifuge units. DNA was quantified at 260 nm using a Varian Cary 300 Bio UV-Vis spectrophotometer.

DNase I assay and analysis

For each assay, 5'-Fluorescein modified aptamer and FB_1 were incubated for 30 min on a vortex shaker at room temperature. FB_1 was gratefully acquired from Dr. David Miller (Carleton University, Ottawa, Canada). The conditions for the DNase I assay are summarized in Table 2.

DNase I (New England BioLabs) was added, briefly vortexed to ensure complete mixing, and incubated at 37°C for precisely 60 seconds in a heat block. DNase I digestion was stopped with the addition of 1 µl 0.5 M EDTA at 90°C, vortexed to mix, and immediately heat deactivated at 90°C for 10 minutes. The samples were mixed 1:1 with formamide and heated at 55°C for 5 minutes prior to separation for 3 hours at 300 V on a 19% denaturing PAGE gel in a SE 600 Chroma Standard Dual gel electrophoresis unit. Gels were visualized with the fluorescent setting (302 nm) in an AlphaImager Multi Image Light Cabinet (Alpha Innotech).

	FB_1 (nM)	FB_1 (µl) (range of conc.)	DNA 50 µM (µl)	DNase I (µl)	DNase I Rxn Buffer (µl)
1	N/A	0	10	0	92
2	N/A	0	10	1	90
3	0.1	10	10	1	80
4	1	10	10	1	80
5	10	10	10	1	80
6	100	10	10	1	80
7	1 000	10	10	1	80
8	10 000	10	10	1	80

Table 2. Reaction conditions for DNase I digestion assay. DNase I Reaction Buffer (10 mM Tris-HCl, 2.5 mM $MgCl_2$, 0.5 mM $CaCl_2$ pH 7.0)

Fluorescent digestion bands were quantified using the SpotDenso program on the AlphaImager. Each band produced from the digestion was calculated as a ratio relative to the entire sample to avoid any errors stemming from loading discrepancies. The density of each band (A, B, C, etc.) relative to FB_1 concentration (log of 0.1 nM – 10 µM) was plotted with GraphPad Prism non-linear regression one-site specific binding [1] (GraphPad Prism version 5.00, GraphPad Software, San Diego California, USA, www.graphpad,com).

[1] $$Y = (B_{max})(X)/(K_d + X)$$

Digestions bands that showed a change in intensity relative to FB_1 concentration produce a binding isotherm (K_d) with an associated standard error.

Variable temperature UV-Visible spectroscopy

Melting studies were performed with a Varian Cary 300 Bio UV-Visible Spectrophotometer equipped with a 6x6 Peltier-Thermostatted Multicell Holder. 3 ml of 5'-fluorescein labeled aptamers (~2 µM) in FB_1 selection buffer (100 mM NaCl, 20 mM Tris, 2 mM $MgCl_2$, 5 mM KCl, 1 mM $CaCl_2$, pH 7.6). Absorbance was monitored at 260 nm over three temperature ramps (Ramp 1 80°C - 20°C; Ramp 2 20°C - 80°C; Ramp 3 80°C - 20°C). The ramp rate was 0.5°C/min with a 5 minute hold between each temperature change. Melting temperatures were determined by fitting the change in absorbance at 260 nm relative to temperature using Standard Curves Analysis on SigmaPlot.

Magnetic Bead conjugation with FB_1

NH_2-Dynabeads® M-270 Amine (Life Technologies) are superparamagnetic and allow for efficient separation of beads from solution when placed in a DynaMag-2 magnet. Beads were suspended in PBS buffer (137 mM NaCl, 2.7 mM KCl, 10 mM Na_2HPO_4, 1.8 mM KH_2PO_4, pH 7.4) at 30 mg/ml and washed three times with buffer, separating on the magnet each time. The beads were re-suspended in 5% glutaraldehyde (Sigma Aldrich) in PBS buffer, and incubated for 2 hours at room temperature on a vortex shaker. Control beads were incubated without glutaraldehyde. The beads were again washed three times with PBS buffer, resuspended in 20 µM FB_1 in buffer, and incubated at room temperature on a vortex shaker overnight. After three buffer washes to remove unbound FB_1, unbound NH_2 groups on the bead surface were capped with a 20 mg/ml solution of Sulfo-NHS Acetate (Thermo Scientific) in buffer, incubated for two hours at room temperature on a vortex shaker. The beads were again washed three times with buffer, and stored at 4°C.

Magnetic Bead assay for determining aptamer affinity

5'-fluorescein modified aptamers were pre-heated at 90°C for 10 min and room temperature for >30 min prior to the binding assay. FB_1-conjugated beads prepared as above were washed three times in binding buffer prior to the assay. For each assay, six concentrations of aptamer were tested ($1x10^{-6}$, $5x10^{-7}$, $2x10^{-7}$, $1x10^{-7}$, $5x10^{-8}$, and $2x10^{-8}$ M) in 100 µl total volume of beads at 30 mg/ml in binding buffer. The beads and aptamers

were incubated for 60 min at room temperature on a vortex shaker. Beads were placed on the DynaMag-2 magnet, and four 100 µl washes of buffer at room temperature were collected to remove non-binding aptamer. Three 100 µl washes were obtained by incubating the beads at 90°C for 10 min to elute binding aptamer. All washes were quantified on a Fluorescence Spectrophotometer (Horiba Jobin Yvon, USA) with SpectrAcq controller. Fluorescein-modified aptamer was excited at 494 nm and an emission spectra of 500 – 600 nm was collected. The amount of total aptamer in each wash was quantified by comparing the fluorescence intensity to standards of known aptamer concentrations. For each sample ($1x10^{-6}$, $5x10^{-7}$, $2x10^{-7}$, $1x10^{-7}$, $5x10^{-8}$, and $2x10^{-8}$ M) the total amount of aptamer bound was quantified. K_d binding isotherms were generated using GraphPad Prism non-linear regression one-site specific binding analysis.

Conclusions

We describe for the first time a novel application of the DNase I digestion assay to study the structure and affinity of aptamers binding to small molecule targets. We validated our assay using a previously described aptamer that bound to the important mycotoxin FB_1. This assay is a cheap, simple method to screen aptamers for regions of important structural motifs, and to characterize which regions within the aptamer are affected by target binding. This approach is applicable for screening multiple sequences and can be applied towards the rational design and testing of minimer sequences. Importantly, this method is one of the few methods that permits the measurement of aptamer-small molecule binding in solution. This makes this method generally applicable to all small molecule aptamers and furthermore, provides a more realistic understanding of the aptamer-target interaction for downstream sensor applications that would also require target free in solution.

Using these assay, we discovered that the truncated aptamers *FB1_39t3* and *FB1_39t3-5* demonstrated displayed comparable high affinity binding to FB_1 relative to the full-length aptamer. We verified this finding using a traditional magnetic bead assay. These new truncated and validated aptamers can now be directly implemented into novel biosensor platforms permitting rapid and inexpensive detection of this important toxin in the field.

Acknowledgements

The authors thank the Natural Science Engineering Research Council of Canada (NSERC) for a Discovery Grant (MCD), PGS-M (NRF), and PDF (MM) funding. MCD also thanks the Western Grains Research Foundation for funding.

Notes and references

1 M. Famulok, G. Mayer, *Acc Chem Res,* 2011, **44,** 1349-1358.
2 M. McKeague, M.C. DeRosa, *J Nucleics Acids,* 2012, **2012**, 748913.
3 S. Li, D. Chen, Q. Zhou, W. Wang, L, Gao, J. Jiang, H. Liang, Y. Liu, G. Liang, H. Cui, *Anal Chem,* 2014, **86,** 5559-5566.
4 Y. Miyachi, C. Ogino, A. Kondo, 2014, *Nucleosides, Nucleotides and Nucleic Acids,* **33**, 31-39.
5 P.H. Lin, R.H. Chen, C.H. Lee, Y. Chang, C.S. Chen, W.Y. Chen, 2011, *Colloids and Surfaces B: Biointerfaces,* **88**, 552-558.
6 O. Reinstein, M. Yoo, C. Han, T. Palmo, S.A. Beckham, M.C.J. WIlce, P.E. Johnson, 2013, *Biochemistry,* **52**, 8652-8662.
7 Y. Ding, X. Zhang, K.W. Tham, P.Z. Qin, *Nucleic Acids Research,* 2014, **42**, 140.
8 S. Bellaousov, J.S. Reuter, M.G. Seetin, D.H. Mathews, *Nucleic Acids Research,* 2013, **41**, 471-474.
9 J.S. Reuter, D.H. Mathews, *BMC Bioinformatics,* 2010, **11**, 1-9.
10 D.H. Mathews, W.N. Moss, D.H. Turner, *Cold Spring Harb Perspec Biol,* 2010, **2**, a003665
11 L. Jiang, D.J. Patel, *Nature Structural Biology,* 1998, **5**, 769-774.
12 V.J.B Ruigrok, M. Levisson, J. Hekelaar, H. Smidt, B.W. Dijkstra, J. van der Oost, *Int J Mol Sci,* 2012, **13**, 10537-10552.
13 O. Reinstein, M.A.D. Neves, M. Saad, S.N. Boodram, S. Lombardo, S.A. Beckham, J. Brouwer, G.F. Audete, P. Groves, M.C.J. Wilce, P.E. Johnson, *Biochemistry,* 2011, **50**, 9368-9376.
14 B.M. McGrath, G. Walsh, *CRG Press,* 2005, ISBN 978-0-8493-2714-8.
15 K.D. Connaghan-Jones, A.D. Moody, D.L. Bain, *Nat Protoc,* 2008, **3**, 900-914.
16 M. Brenowitz, D.F. Senear, R.E. Kingston, *Current Protocols in Molecular Biology,* 1989, 12.4.1-12.4.16.
17 T.D. Tullius, *Annu Rev Biophys Biophys Chem,* 1989, **18**, 213-237.
18 M. Zianni, K. Tessanne, M. Merighi, R. Laguana, F.R. Tabita, *J Biomolecular Techniques,* 2006, **17**, 103-113.
19 M. Wongphatcharachai, P. Wang, S. Enomoto, R.J. Webby, M.R. Gramer, A. Amison, S. Sreevatsan, *Journal of Clinical Microbiology,* 2012, **51**, 46-54.
20 R.D. Walters, D.T. McSwiggen, J.A. Goodrich, J.F. Kugel, *Plos ONE,* 2014, **9**, e101015.
21 R. Joshi, H. Janagama, H.P. Dwivedi, T.M.A. Senthil Kumar, L.A. Jaykus, J. Schefers, S. Sreevatsan, *Molecular and Cellular Probes,* 2009, **23**, 20-28.
22 R.J. White, A.A. Rowe, K.W. Plaxco, *Analyst,* 2010, **135**, 589-594.
23 P. Burgstaller, M. Kochoyan, M. Famulok, *Nucleic Acids Research,* 1995, **23**, 4769-4776.
24 G.S. Shephard, M.E. Kimanya, K.A. Kpodo, G.J. Benoit Gnonlonfin, W.C.A. Gelderblom, *Food Control,* 2013, **34**, 596-600.
25 K.A. Voss, G.W. Smith, W.M. Haschek, *Animal Feed Science and Technology,* 2007, **137**, 299-325.
26 H. Stockmann-Juvala, K. Savolainen, *Human and Experimental Toxicology,* 2008, **27**, 799-809.
27 W.F.O. Marasas, R.T. Riley, K.A. Hendricks, V.L. Stevens, T.W. Sadler, J. Gelineau-van Waes, S.A. Missmer, J. Cabrera, *Journal of Nutrition,* 2004, **134**, 711-716.
28 J.D. Miller, A.W. Schaafsma, D. Bhatnagar, G. Bondy, I. Carbone, L.J. Harris, G. Harrison, G.P. Munkvold, I.P. Oswald, J.J. Petska, L. Sharpe, M.W. Sumarah, S.A. Tittlemeir, T. Zhou, *World Mycotoxin Journal,* 2013, **1**, 63-82.
29 A. Visconti, M. Solfrizzo, A. De Girolamo, *Food Chemical Contaminants,* 2001, **84**, 1828-1838.
30 L. Dasko, D. Rauova, E. Belajova, M. Kovac, *Czech Journal of Food Science,* 2005, **23**, 20-26.
31 S. Ling, J. Pang, J. Yu, R. Wang, L. Liu, Y. Ma, Y. Zhang, N. Jin, S. Wang, *Toxicon,* 2014, **80**, 64-72.

32 Z.Q. Hu, H.P. Li, P. Wu, Y.B. Li, Z.Q. Zhou, J.B. Zhang, J.L. Liu, Y.C. Liao, *Analytia Chimica Acta,* 2015, **867**, 74-82.
33 E. Bowers, R. Hellmich, G. Munkvold, *Journal of Agricultural Food Chemistry,* 2014, **62**, 6463-6472.
34 M. McKeague, C.R. Bradley, A. De Girolamo, A. Visconti, J.D. Miller, M.C. DeRosa, *Int J Mol Sci*, 2010, **11**, 4864-4881.
35 X. Chen, Y, Huang, N. Duan, S. Wu, Y. Xia, X. Ma, C. Zhu, Y. Jiang, Z. Ding, Z. Wang, *Microchimica Acta,* 2014, **181**, 1317-1324.
36 S. Wu, N. Duon, X. Ma, Y. Xia, H. Wang, Z. Wang, Q. Zhang, *Analyst,* 2012, **84**, 6263-6270.
37 S. Wu, N. Duan, X. Li, G. Tan, X. Ma, Y, Xia, Z. Wang, H. Wang, *Talanta,* 2013, **116**, 611-618.
38 S. Yue, X. Jie, L. Wei, C. Bin, W. Dou Dou, Y. Yi, L. QingXia, L. JianLin, Z. TieSong, *Anal Chem,* 2014, **86**, 11797-11802.
39 X. Chen, X. Bai, H. Li, B. Zhang, *RCS Advances,* 2015, **5**, 35448-35452.
40 M. McKeague, R. Velu, K. Hill, V. Bardoczy, T. Meszaros, M.C. DeRosa, *Toxins,* 2014, **6**, 2435-2452.